Biochemistry and Biophysics Reports 11 (2017) 112–118

Contents lists available at ScienceDirect

Biochemistry and Biophysics Reports

journal homepage: www.elsevier.com/locate/bbrep

Insight into the binding of a non-toxic, self-assembling aromatic tripeptide with ct-DNA: Spectroscopic and viscositic studies

Soumi Biswas[a], Satyabrata Samui[a], Arpita Chakraborty[a], Sagar Biswas[b], Debapriya De[a], Utpal Ghosh[a], Apurba K. Das[b], Jishu Naskar[a,*]

[a] Department of Biochemistry & Biophysics, University of Kalyani, Nadia, WB 741235, India
[b] Department of Chemistry, Indian Institute of Technology, Indore, Khandwa Road, Indore 453552, India

ARTICLE INFO

Keywords:
Peptide
Self-assembly
ct-DNA
Hyperchromism
Groove binding

ABSTRACT

The report describes the synthesis, self-association and DNA binding studies of an aromatic tripeptide H-Phe-Phe-Phe-OH (FFF). The peptide backbone adopts β—sheet conformation both in solid and solution. In aqueous solution, FFF self-assembles to form nanostructured aggregates. Interactions of this peptide with calf-thymus DNA (ct-DNA) have been studied using various biophysical techniques including ultraviolet (UV) absorption spectroscopy, fluorescence spectroscopy and circular dichroism (CD) spectroscopy. The value of mean binding constant calculated from UV and fluorescence spectroscopic data is $(2.914 \pm 0.74) \times 10^3\ M^{-1}$ which is consistent with an external binding mode. Fluorescence intercalator displacement (FID) assay, iodide quenching study, viscosity measurement and thermal denaturation study of DNA further confirm the groove binding mode of peptide, FFF with ct-DNA. MTT cell survival assay reveals very low cytotoxicity of the peptide toward human lung carcinoma cell line A549.

1. Introduction

In recent years, peptide-based biomaterials have drawn immense attention to the scientific community owing to their various functional activities in different areas including drug delivery [1a-f], tissue engineering [1g], bio-diagnostic tool [1h], antibiotic [1i-j] and regenerative medicine [1k]. The structural and chemical diversity of peptides, in addition to their ability to adopt the specific secondary structure, provide a unique bottom-up platform for the construction of nanomaterials [2]. A number of peptide-based building blocks, such as cyclic peptides [3], amphiphilic peptides [4], co-polypeptides [5], dendritic peptides [6], and aromatic dipeptides have been reported which can form various supramolecular structures having applications in biology and nanotechnology. Among these structural building blocks, an aromatic dipeptide diphenylalanine (H-Phe-Phe-OH, FF) is most extensively studied. Diphenylalanine produces nanotubes which could serve as casts for the formation of silver nanowires with the average diameter of 20 nm [7]. FF nanotubes have unique chemical and thermal stability, as well as exhibit excellent mechanical properties [8]. Synthesis of D-Phe-D-Phe based peptide-nanotube-platinum nanoparticles composite was reported by Song et al. [9] Fluorenylmethyloxycarbonyl (Fmoc) protected diphenylalanine (Fmoc-Phe-Phe-OH) has been used for the formation of nanofibrous hydrogel with notable physical and mechanical properties [10]. It can support the cell growth and release the entrapped small molecules in a controlled manner. Fmoc-Phe-Phe-OH has also been used for the formation of hydrogel nanoparticles (HNPs) which has the ability to deliver various drugs and bioactive molecules [10c]. Li et al. reported concentration dependent reversible shape transition between self-assembled cationic dipeptide (H-Phe-Phe-NH_2) nanotubes and vesicle-like structures [11]. Moreover, the self-assembled positively charged nanotubes can bind with fluorescently labeled ssDNA using electrostatic interactions and also enter into the cells readily. Furthermore, the glycopeptide conjugates (conjugation of FF dipeptide with several saccharides) adopt various structures and increased solubility in the aqueous medium compared to the original diphenylalanine building block. The increased solubility and different nanostructures pave the way for new applications in the aqueous environment [12]. The morphology of the FF assemblies could be fine-tuned and tailored by various factors such as pH, substrate roughness, hydrophobicity, temperature and ionic strength which make it a promising candidate for *in vivo* biological applications [13]. In 2013, Bosne et al. reported that FF peptide nanotubes exhibit piezoelectric effect [14a]. Nmoc-F/FF (Nmoc: naphthalene-2-methoxycarbonyl) system has been used to generate Nmoc-Phe-Phe-Phe-OH as a preferred product in the protease catalysed dynamic peptide library [14b]. The self-assembled tripeptide Boc-FFF based bionanospheres

* Corresponding author.
E-mail address: jishunaskar@gmail.com (J. Naskar).

http://dx.doi.org/10.1016/j.bbrep.2017.07.001
Received 19 May 2017; Received in revised form 28 June 2017; Accepted 1 July 2017
Available online 08 July 2017

have been used in conventional device-fabrication processes using nanolithography [14c].

Here, we explore the aptitude of an aromatic tripeptide H-Phe-Phe-Phe-OH (FFF) as DNA molecular probe which deserves much attention for the development of DNA-targeting drugs and new therapeutics. Previously, it was reported that FFF has higher network propensities and FFF aggregates are more stable than FF networks [15]. Our results clearly show that the aromatic tripeptide FFF forms nanostructured aggregates upon self-association in aqueous solution. Moreover, ultraviolet (UV) absorption spectroscopy, fluorescence spectroscopy, circular dichroism (CD) study, viscosity measurement and thermal denaturation analysis of DNA indicate that FFF binds with ct-DNA presumably *via* groove binding manner. Finally, the cytotoxicity of this tripeptide has been tested by MTT cell survival assay using human lung carcinoma cell line A549.

2. Results and discussion

2.1. Conformational analysis

Information regarding the conformation of the peptide in solid state has been obtained from Fourier Transform Infrared (FT-IR) spectroscopy. FT-IR spectrum of the peptide in the solid state shows a well defined C=O stretching band (amide I) at 1648 cm^{-1} and N—H stretching band at 3380 cm^{-1} (Fig. S10), typical of intermolecularly hydrogen-bonded β—sheet structure in the solid state [16a]. Moreover, N—H bending frequency of this peptide appears at 1518 cm^{-1} suggesting also the formation of β-sheet structure in the solid state [16b]. Conformational analysis of the peptide in solution has been done by NMR spectroscopy. ^{1}H NMR coupling constants provide information about the conformation of the peptide main chain. The vicinal coupling constant between NH and $C^{\alpha}H$ of a peptide ($^3J_{HN\alpha}$) reflects the dihedral angle between these two protons, and hence the main chain φ—angle. Coupling constants ($^3J_{HN\alpha}$) greater than 7 Hz are consistent with β-sheet structure, while coupling constants less than 6 Hz are consistent with α-helical structure [17a]. From NMR study of the peptide in DMSO-d_6, it is found that the value of $^3J_{HN\alpha}$ for Phe(2) and Phe(3) residues is 8 Hz (Fig. S6), clearly indicating β-sheet conformation of the peptide in solution. Further to analyze the conformation of the peptide in solution, CD spectroscopy has been studied. Fig. S18 is the CD spectrum of the peptide in water. From the spectral data, it is estimated that, β-sheet content of the peptide in solution is 52.93% following the method reported by Perez-Iratxeta et al. [17b]

2.2. Self-association study

The formation of supramolecular structures through molecular self-assembly was primarily accessed by dynamic light scattering (DLS) study. It is frequently used to determine the size distribution profile of small particles or assemblies in solution. From the DLS study, it is found that nanostructures of various sizes are formed (Fig. S11) at a peptide concentration of 0.82 mg mL^{-1}. The average size (hydrodynamic diameter) of the aggregate is found to be 930 nm. This observation encouraged us to further study these structures by electron microscope. Transmission electron microscopic (TEM) study has been performed to reveal the morphology of these self-assembled structures. The experiment was done at 1.57 mg mL^{-1} concentration of peptide. The images (Fig. 1a and Fig. S12a) prove the formation of 'nanosheet' like aggregates which is very much similar with the report of Tamamis et al. [15] The width of the sheets are in the range from 1.8 to 26.1 nm. Moreover, the high resolution TEM images reveal that each 'nanosheet' consists of several small fibril-like aggregates having average diameter of 0.95 nm (Fig. 1b and Fig. S12b).

2.3. DNA binding study

DNA is one of the important intracellular targets for a wide range of anticancer and antibiotic drugs. The binding between small molecules and DNA is very much important for rational design of new drugs for clinical use. Recently, a growing emphasis has been placed on binding studies of small molecules [18a,b,c,d,e] and nanoparticles [18f,g,h,i,j,k] with DNA, but interactions specificity of small synthetic peptide containing consecutive aromatic amino acid residues is relatively less explored [19]. Here, we have studied the interactions of FFF with calf thymus DNA (ct-DNA) by various techniques including ultraviolet (UV) absorption spectroscopy, fluorescence spectroscopy, circular dichroism (CD) study, viscosity measurement, and thermal denaturation study of DNA.

2.4. UV absorption study

UV absorption measurement is a very efficient method to perceive the binding of small molecules with DNA by monitoring the changes of absorption properties of either interacting molecules or DNA. In general, when the binding mode is through intercalation then it results in both hypochromism and bathochromism [18e]. On the other hand, hyperchromism indicates the partial or non-intercalative binding modes, such as electrostatic forces, van der Waals interactions, dative bonds, hydrogen bonds and hydrophobic interactions [20]. The absorption spectra of ct-DNA upon gradual addition of peptide have been shown in Fig. S13. From the titration study, it was observed that, the intensity of absorption maxima at 258 nm increased gradually upon addition of peptide without any shift of absorption band which clearly indicates the non-intercalative binding of peptide with ct-DNA [18e]. The value of binding constant K_b, is calculated from the spectral data using double reciprocal plot following the equation:

$$\frac{1}{A_0 - A} = \frac{1}{A_0} + \frac{1}{A_0 C K_b}$$

where A_0 is the absorbance of ct-DNA at 258 nm in the absence of peptide and A is the recorded absorbance of ct-DNA in presence of different concentration of peptide, C is the concentration of peptide and K_b is the binding constant. The plot of $1/(A_0\text{-}A)$ against $1/C$ is found (Fig. S14) to be linear ($R^2 = 0.976$) and the value of K_b is calculated to be $3.801 \times 10^3\ M^{-1}$ from the slope of the plot.

2.5. Fluorescence study

The change in fluorescence spectral intensities is often employed to assess the binding of ligand with DNA. The fluorescence behavior of the peptide was monitored in presence of various concentration of DNA upon excitation at 257 nm. From the emission spectra (Fig. 2a), it was observed that the fluorescence intensity of peptide decreased gradually upon progressive addition of ct-DNA. Furthermore, fluorescence titration data have been used to determine the binding constant (K) and the binding stoichiometry (n) for the interaction of peptide with ct-DNA using the following equation:

$$\log \frac{F_0 - F}{F} = \log K + n \log [DNA]$$

where, F_0 and F are the fluorescence intensities of peptide in absence and presence of different concentrations of ct-DNA. K and n are the binding constant and binding stoichiometry respectively. Fig. 2b shows that the plot of $\log \{(F_0\text{-}F)/F\}$ *vs* log[DNA] is linear with R^2 value 0.96924. From the plot, calculated binding constant value is $2.028 \times 10^3\ M^{-1}$ which is in good agreement with the binding constant value obtained from UV absorption study. The value of n is found to be 1.26.

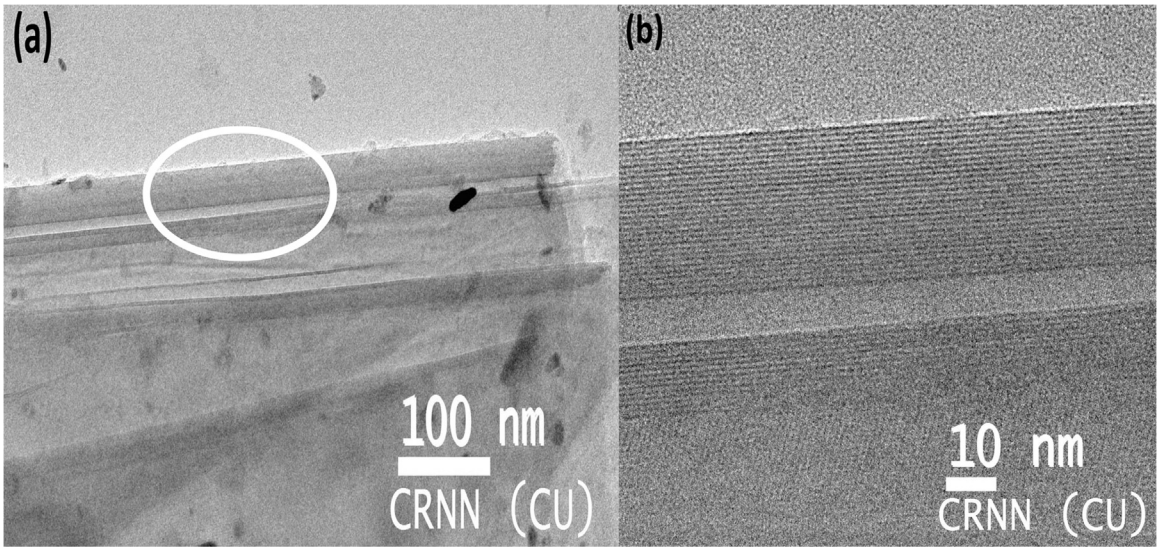

Fig. 1. TEM images of peptide at concentration 1.57 mg/mL. Image (a) shows the formation of 'nanosheet' and (b) magnified image of the circle region showing that each 'nanosheet' consist of several small fibrils like aggregate.

2.6. Fluorescence intercalator displacement (FID) assay

Ethidium bromide (EB) is a well-known intercalator which is often used as a spectral probe to establish the mode of binding of small molecules to double-helical DNA [21a,b,c,d]. The fluorescence intensity of EB increases after binding with DNA due to intercalation. Like EB, if peptide intercalates into the helix of DNA, it would compete with EB for the intercalation sites in DNA, and leads to a significant decrease in the fluorescence intensity of EB–DNA complex. In this regard, 50% decrease in fluorescence intensity has been reported for an intercalator lucigenin [21c]. To access whether peptide can intercalate into the helix of DNA, EB-DNA complex was titrated with various concentrations of peptide. From the titration curve (Fig. S15) no significant decrease in fluorescence intensity of EB-DNA complex was observed. This result indicates that the peptide can't displace EB from the EB-DNA complex *i.e.* peptide is not an intercalator.

2.7. Effect of ionic strength

In order to prove, whether electrostatic interaction is playing a prevalent role in the binding of peptide with ct-DNA, the effect of different concentration of NaCl (from 0.01 to 0.35 mol L^{-1}) on the fluorescence intensity of peptide and peptide–ct-DNA complex were investigated. NaCl is not anionic quencher of DNA [21e,f] rather it could compete for phosphate anion [21g]. If the compound binds to DNA through an electrostatic interaction, the surface of DNA will be surrounded by the sodium ions with the increase of ionic strength. Then it is difficult for peptide to approach DNA and the strength of interaction between peptide and DNA decreases, as a result the degree of fluorescence quenching also falls. From the titration study (Fig. 3) it is clear that the addition of NaCl have no significant effect on the fluorescence intensity of peptide and peptide-ctDNA complex, which suggest that the electrostatic mode of binding between peptide and ct-DNA could be ruled out.

2.8. KI quenching study

In order to establish the mode of binding between peptide and ct-DNA, fluorescence quenching in absence and presence of ct-DNA was studied using potassium iodide (KI) as a quencher [22a]. Iodide ion is negatively charged quencher that can effectively quench the fluorescence of small molecules in aqueous medium. Science DNA contains negatively charged phosphate backbone, so it repels anionic quencher. Therefore, fluorescence intensity of an intercalating small molecule is well protected from being quenched as the approach of anionic quenchers towards the fluorophore is restricted [22b]. However, groove binding provides very little protection for the fluorophore as it remains expose to the external environment and iodide anions can readily quench their fluorescence even in presence of DNA [18b]. In order to elucidate the mode of binding of peptide with ct-DNA, the fluorescence

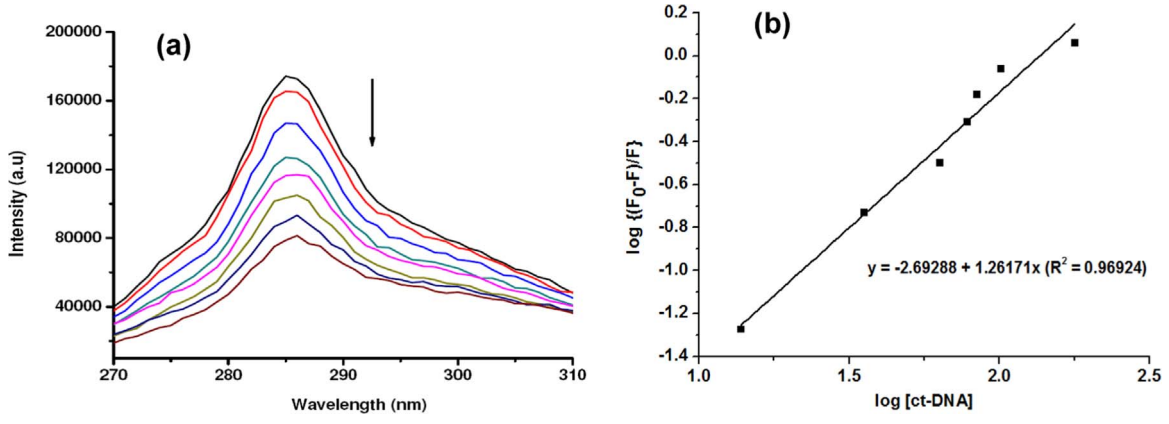

Fig. 2. Fluorescence titration study of peptide with ct-DNA. (a) Gradual addition of ct-DNA into peptide leads to a decrease in fluorescence intensity of peptide at 285 nm. Here, amount of peptide was kept constant at 40.8 μM and DNA concentrations were varied from 0 to 178.53 μM. (b) The plot of log{(F_0-F)/F} *vs* log [ct-DNA] is found to be linear with R^2 value 0.96924.

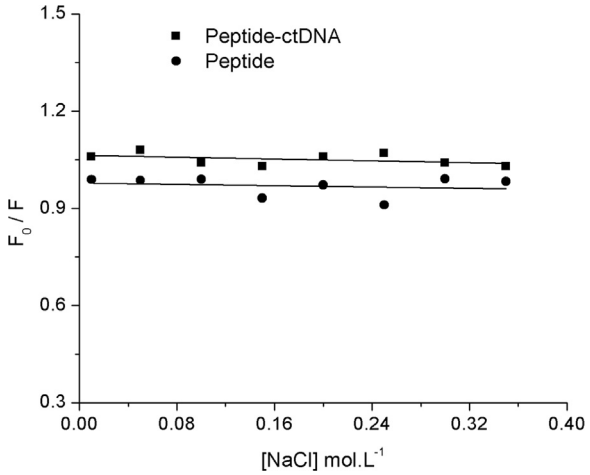

Fig. 3. Effect of ionic strength on the fluorescence intensity of peptide and peptide–ct-DNA complex. Here [peptide] = 6.4 μM, [ct-DNA] = 12.10 μM and [NaCl] = 0.01, 0.05, 0.10, 0.15, 0.20, 0.25, 0.30, 0.35 mol/L. F_0 and F indicate the fluorescence intensity in absence and presence of NaCl.

quenching of peptide in absence and presence of ct-DNA was studied using various concentration of KI. The quenching constants (K_{sv}) were calculated by using Stern-Volmer equation (Fig. 4). The quenching constants (K_{sv}) for free peptide and peptide–ct-DNA complex were calculated to be 204.6 and 199.8 L mol^{-1} respectively. These comparable values indicate that almost similar aqueous environment persist around peptide before and after binding with ct-DNA, *i.e.* groove binding mode is operating between peptide and ct-DNA.

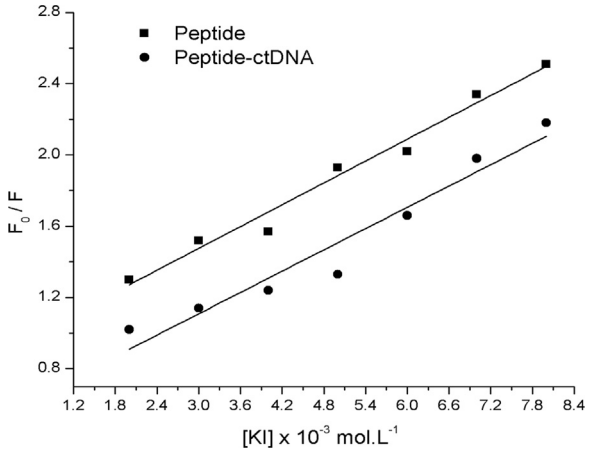

Fig. 4. Fluorescence quenching plots of peptide by KI in absence and presence of ct-DNA at pH 7.4. Here [peptide] = 80 μM, [ct-DNA] = 120 μM and [KI] = (2–8) × 10^{-3} mol L^{-1}. F_0 and F indicate the fluorescence intensity in absence and presence of KI.

2.9. CD study

The effect of peptide on the conformation of secondary structure of ct-DNA was investigated by circular dichroism (CD) study. Keeping the concentration of DNA fixed at 15 μM, the peptide concentrations were varied from 0 to 30 μM. The ct-DNA in the B conformation shows two conservative CD bands in the ultraviolet (UV) region. A positive band appears at 273 nm due to base stacking whether a negative band appears at 245 nm due to the presence of polynucleotide helicity [21c,22c]. From the CD study, it was found (Fig. 5) that the ellipticity of the negative band was decreased significantly upon progressive addition of peptide. Such CD spectral changes clearly indicate that the binding of peptide with ct-DNA leads to a slight perturbation in the conformation of secondary structure of ct-DNA.

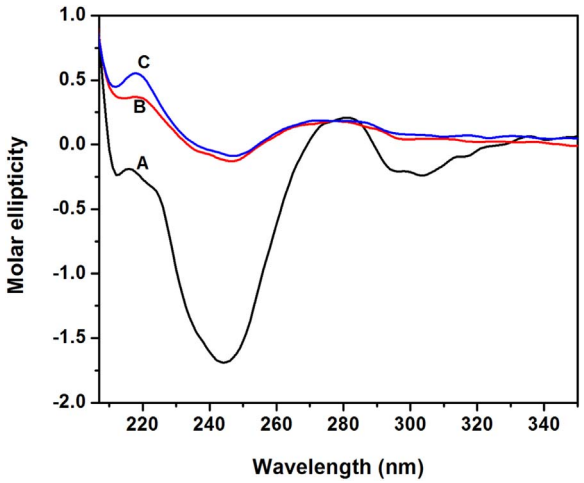

Fig. 5. CD signature of the peptide–ct-DNA interaction. The normalized CD spectra of ct-DNA in absence of peptide (A), in presence of 15 μM (B) and 30 μM concentration of peptide (C). ct-DNA concentration was fixed at 15 μM.

2.10. Viscosity study

Viscometry is an effective tool to determine the mechanism of interaction of small molecules with ct-DNA at molecular level. Classical intercalative mode usually reflects an increase in the viscosity of ct-DNA due to the separation of base pairs at the intercalation sites, whereas the molecules that binds in the DNA grooves by partial or non-classical intercalation causes less positive or negative or no change in the viscosity of DNA [22c]. Therefore, to further clarify the mode of binding of peptide to ct-DNA, changes in viscosity of ct-DNA solutions were measured in presence of various concentration of peptide at 25 °C. The values of relative viscosity $(\eta/\eta_0)^{1/3}$ was plotted against R (R = [peptide]/[ct-DNA]). From the plot (Fig. 6), it is clear that viscosity of ct-DNA solutions remain almost steady upon gradual addition of peptide which suggests the groove binding mode of interaction between peptide and ct-DNA.

2.11. Thermal denaturation analysis of DNA

Thermal denaturation of DNA provides a convenient tool for the detection of binding and assessing the relative strength of binding between ligand and DNA. It is well known that when temperature is raised, the double-stranded DNA gradually dissociates into single strands. The DNA melting temperature (T_m) is defined as the temperature where half of the total base pairs are unbound [21d,22c]. It is

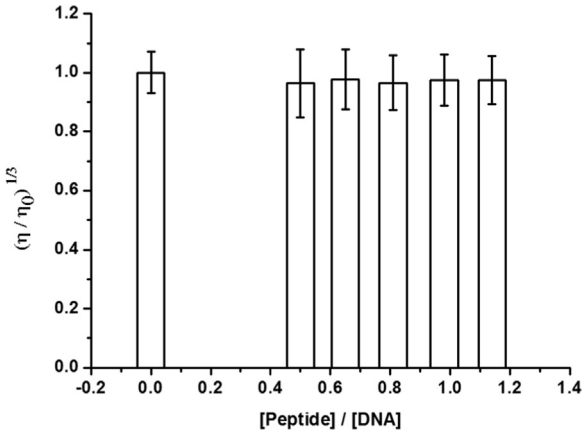

Fig. 6. Effect of increasing amount of peptide (0–253 μM) on relative viscosity of ct-DNA at 25 °C. [DNA] = 221 μM. Values reported here are mean of three independent experiments.

determined by plotting the absorbance of DNA at 260 nm as a function of temperature. Generally, intercalation of small molecules into the double helix of DNA causes stabilization of base stacking and leads to a significant increase (about 5–8 °C) in melting temperature (T_m) of the double-stranded DNA, while non-intercalation binding causes no obvious increase in T_m [23]. The melting curves of the ct-DNA in absence and presence of peptide are illustrated in Fig. 7. The T_m of ct-DNA in absence of peptide was calculated to be 80.18 °C and it reduced to 77.86 °C in presence of peptide. This small change of T_m suggests that the peptide possibly bind with DNA at the groove, which makes the DNA double helix slightly less stable compared to free DNA.

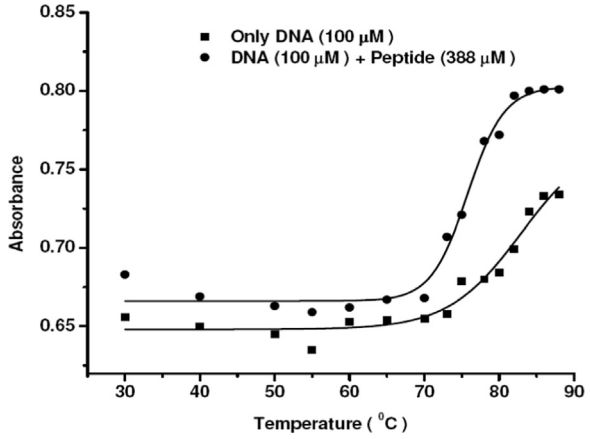

Fig. 7. DNA melting study. Melting temperature of DNA in presence and in absence of peptide were 77.86 °C and 80.18 °C respectively.

2.12. Cytotoxicity assay

MTT cell survival assay was done to test the cytotoxicity of peptide upon treatment on human lung carcinoma cell line A549. The cells were treated with various concentration of peptide for 24 h. No significant decline (Fig. 8) of the percentage of viable cells was observed upon treatment, indicating that the peptide is nontoxic in nature. Interestingly, it was also found that the morphology of cells (Fig. S16) was almost remaining same in case of treatment compared to untreated control.

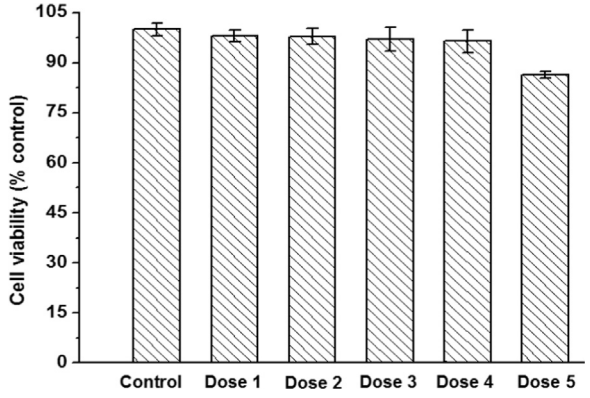

Fig. 8. MTT assay for Cell viability. Cells were treated with different concentration of peptide for 24 h. Here, dose 1–5 indicates peptide concentrations 10, 50, 100, 150 and 200 μM respectively. Values reported here are mean of three independent experiments.

3. Conclusions

Herein, we report the supramolecular assembly of a synthetic aromatic tripeptide H-Phe-Phe-Phe-OH (FFF). The backbone of the peptide adopts β-sheet conformation both in solid and solution. The morphology of the peptide was studied by TEM which reveal the formation of nanosheet-like aggregates having width ranging from 1.8 to 26.1 nm. High resolution TEM images also prove that each 'nanosheet' consists of several small fibril-like aggregates having average diameter of 0.95 nm. The interactions of this peptide with ct-DNA have been studied using various spectroscopic techniques including UV, fluorescence and CD. The mean binding constant is calculated as $(2.914 \pm 0.74) \times 10^3\ M^{-1}$ from UV and fluorescence spectroscopic data which is consistent with an external binding mode. FID assay, iodide quenching study, viscosity measurement and thermal denaturation analysis of DNA further confirm the groove binding mode of peptide with ct-DNA. Finally, MTT cell survival assay proves that the peptide is nontoxic in nature. The study provides a deep insight in the binding mechanism of an aromatic tripeptide with ct-DNA.

4. Experimental section

The amino acid used in the preparation of peptides, coupling reagents dicyclohexylcarbodiimide (DCC) and N-hydroxybenztriazole (HOBt), ethidium bromide (EB), dimethyl sulphoxide (DMSO) used for MTT assay, were purchased from SRL, India. ct-DNA was purchased from Sigma Aldrich. DMEM media, fetal bovine serum, antibiotics, for cell culture and MTT assay, were purchased from HiMedia, India.

The reported peptide was synthesized by conventional solution phase method using racemization-free fragment condensation strategy [24a]. The Boc group was used for N-terminal protection and the C-terminus was protected with a methyl ester. Deprotection of the ester group was performed using the saponification method, and removal of the Boc group was done with trifluoroacetic acid (TFA). Couplings were mediated by DCC/HOBt. Final compound was fully characterized by NMR and IR spectroscopy, and mass spectrometry. NMR studies were carried out on a Brüker AV 400 MHz spectrometer at 300 K. Compound concentrations were in the range 1–10 mM in $CDCl_3$, $(CD_3)_2SO$. Mass spectra were recorded on a Bruker MicrOTOF-Q II mass spectrometer by positive mode electrospray ionization. The IR spectra were examined using a Perkin-Elmer (Model RX1) spectrometer. The solid-state FT-IR measurements were performed using the KBr disc technique.

Purity of the peptide has been checked by High Performance Liquid Chromatography (HPLC). A Dionex HPLC-Ultimate 3000 pump was used to analyze the purity of FFF and Boc-FFF-OMe. A 20 μl of sample was injected onto a Dionex Acclaim ® 120 C18 column of 250 mm length with an internal diameter of 4.6 mm and 5 mm fused silica particles at a flow rate of 1 mL min^{-1} (linear gradient of 55% (v/v) acetonitrile in water for 35 min, gradually rising to 100% (v/v) acetonitrile in water at 35 min). The sample preparation involved mixing of 1 mmol of the solid sample in 1000 μl acetonitrile-water (50:50 mixture) solution containing 0.1% trifluoroacetic acid. The samples were then filtered through a 0.45 μm syringe filter (Whatman, 150 units, 13 mm diameter, 2.7 mm pore size) before injection. The peaks of the compounds were identified by using an Ultimate 3000 RS Variable Wavelength Detector at 254 nm [24b,c,d]. Fig. S17a and S17b are the HPLC chromatograms of FFF and Boc-FFF-OMe respectively.

The DLS study was done in a MALVERN ZS Instrument UK using a solution of peptide having concentration 0.82 mg mL^{-1}.

Peptide solution having concentration of 1.57 mg mL^{-1} was prepared and then aged for 6 h. A drop of this solution was placed on a carbon-coated copper grid (300 meshes) and evaporated. It was dried under vacuum for 10 h. With these grids, TEM study was carried out using a JEOL JEM 2010 electron microscope.

Tris-NaCl EDTA (TNE) buffer was prepared with doubly distilled water and pH was adjusted at 7.4. DNA stock solution was prepared using this TNE buffer and stored at 4 °C. For this DNA solution the ratio of A_{260}:A_{280} was 1.89, indicating that the DNA was sufficiently pure and free from protein. Various concentrations of ct-DNA solution were used in different experiments. In each case, the concentration of DNA in solution was measured spectrophotometrically using a known extinction coefficient (ε) value at 260 nm as 6600 M^{-1} cm^{-1}. Concentrated

working stock solution of peptide was also prepared by dissolving the peptide in TNE buffer and the pH maintained at 7.4. UV spectra were recorded on HITACHI U-2910 spectrophotometer.

Fluorescence spectra of peptide were recorded on a PPI-QM40 Spectrofluorimeter at 25 °C using 1 cm quartz cells. Excitation was fixed at 257 nm and emission spectra were recorded in the range from 270 nm to 310 nm. In case of EB displacement assay, a solution containing 199 μM of EB and 20 μM of DNA was titrated with increasing concentration of peptide from 0 to 700 μM. EB-DNA complex was excited at 480 nm and emission spectra were recorded from 500 to 700 nm.

The effect of NaCl on the fluorescence intensity of free peptide and peptide–ct-DNA system were determined by gradual addition of increasing concentrations of NaCl (0.01–0.35 mol L^{-1}) to a fixed concentration of peptide and peptide-ct-DNA complex at room temperature.

The effect of KI on the fluorescence intensity of free peptide and peptide–ct-DNA system were determined by gradual addition of increasing concentrations of KI (2–8) × 10^{-3} mol L^{-1} to a fixed concentration of peptide and peptide-ct-DNA complex at room temperature. The quenching plots were constructed according to the Stern-Volmer equation

$$F_0/F = 1 + K_{sv}[KI]$$

F_0 and F are the fluorescence intensity in absence and presence of KI. K_{sv} is the quenching constant and [KI] is the concentration of iodide. Plot of F_0/F *vs* [KI] appear to be linear and the values of K_{sv} were calculated from the slop of the plot.

Viscosity measurements were carried out with a Brook field DV-III ultra programmable Rheometer at 25 °C.

The CD spectra of DNA incubated with peptide at molar ratios ([peptide]/[DNA]) of 0:1, 1:1 and 2:1 were measured over a wavelength range of 200–350 nm in the TNE buffer (pH 7.4) at 25 °C. A spectrum of buffer solution was recorded and subtracted from the spectra of DNA and DNA–peptide complex. The experiment was done in a CD spectrometer Jasco J-815.

Cytotoxicity of peptide was measured by MTT assay [25a,b]. Human lung carcinoma cell line A549, used for the study, obtained from National Centre for Cell Sciences, Pune, India. In brief, 3 × 10^3 cells were allowed to grow in 100 μl fresh DMEM medium supplemented with 10% fetal bovine serum (FBS) in 96 well plate at 37 °C in a humified atmosphere of 5% CO_2. After 17 h of incubation cells were treated with different concentrations of peptide (0–200 μM) for 24 h. After treatment medium was discarded. 10 μl of MTT solution (5 mg/mL) was added in each well and incubated for 4 h in CO_2 incubator at dark. Then MTT was discarded and 100 μl DMSO was added. Absorbance was measured at 595 nm in Agilent cary spectrophotometer (Cary 100 UV–Vis).

1.5×10^5 number of A549 cells were allowed to grow in fresh DMEM medium for 17 h. After that, medium was discarded and cells were treated with different concentration of peptide (0–200 μM) for 24 h. Then the cells were washed with PBS once and cell morphology was photographed under normal light microscope (Carl Zeiss, Germany) using 10X filter [25c].

Details synthetic procedure, NMR, MASS, FTIR data have been given in Supporting information.

Acknowledgements

(a) Satyabrata Samui and Sagar Biswas gratefully acknowledges to the University of Kalyani and UGC respectively for their fellowship. JN indebted to (b) Department of Science and Technology (DST), Govt. of India for FIST and PURSE programs, and University Grant Commission (UGC), Govt. of India for the SAP program of the Dept. of Bio-Chem. & Bio-Phys. KU, for providing different instrumental and infrastructural support, (c) Department of Physics, KU, for providing the facility of fluorescence spectrophotometer, (d) UGC (Project No. F. 20-36/2013 (BSR)) and DBT (BT/PR14646/NNT/28/989/2015) for financial support, (e) Prof. T. Basu, Dept. of Bio-Chem. & Bio-Phys, KU for providing the DLS facility, (f) CRNN, CU for TEM facility, and (g) AKD sincerely acknowledges to DST Nanomission (SR/NM/NS-1458/2014) for financial support and SIC, IIT Indore for instrumental facilities.

Appendix A. Transparency document

Transparency document associated with this article can be found in the online version at http://dx.doi.org/10.1016/j.bbrep.2017.07.001.

Appendix B. Supplementary material

Supplementary data associated with this article can be found in the online version at http://dx.doi.org/10.1016/j.bbrep.2017.07.001.

References

[1] (a) Y. Gilad, M. Firer, G. Gellerman, Biomedicines 4 (2) (2016) 11, http://dx.doi.org/10.3390/biomedicines4020011;
(b) B. Law, R. Weissleder, C.H. Tung, Biomacromolecules 7 (2006) 1261–1265;
(c) J. Naskar, G. Palui, A. Banerjee, J. Phys. Chem. B 113 (35) (2009) 11787–11792;
(d) N. Habibi, N. Kamaly, A. Memic, H. Shafiee, Nano Today 11 (2016) 41–60;
(e) A. Mishra, J.J. Panda, A. Basu, V.S. Chauhan, Langmuir 24 (2008) 4571–4576;
(f) J.J. Panda, A. Varshney, V.S. Chauhan, J. Nanobiotechnol. 11 (2013) 18;
(g) T.C. Holmes, Trends Biotechnol. 20 (1) (2002) 16–41;
(h) W. Cai, X. Chen, Small 3 (11) (2007) 1840–1854;
(i) R.E.W. Hancock, Lancet 349 (1997) 418–422;
(j) M.D. Seo, H.S. Won, J.H. Kim, T.M. Ochir, B.J. Lee, Molecules 17 (2012) 12276–12286;
(k) J. Boekhoven, S.I. Stupp, Adv. Mater. 26 (2014) 1642–1659.

[2] (a) G. Rosenman, P. Beker, I. Koren, M. Yevnin, B. Bank-Srour, E. Mishina, S. Semin, J. Pept. Sci. 17 (2011) 75–87;
(b) E.D. Santis, M.G. Ryadnov, Chem. Soc. Rev. 44 (2015) 8288–8300;
(c) H. Cui, M.J. Webber, S.I. Stupp, Biopolymers 94 (1) (2010) 1–18;
(d) S. Scanlon, A. Aggeli, Nanotoday 3 (2008) 22–30;
(e) B. Adhikari, A. Banerjee, J. Indian Inst. Sci. 91 (2011) 471–484.

[3] (a) M.R. Ghadiri, J.R. Granja, R.A. Milligan, D.E. McRee, N. Khazanovich, Nature 366 (1993) 324–327;
(b) M.R. Ghadiri, J.R. Granja, L.K. Buehler, Nature 369 (1994) 301–304;
(c) J.D. Hartgerink, J.R. Granja, R.A. Milligan, M.R. Ghadiri, J. Am. Chem. Soc. 118 (1996) 43–50;
(d) S. Fernandez-Lopez, H.S. Kim, E.C. Choi, M. Delgado, J.R. Granja, A. Khasanov, K. Kraehenbuehl, G. Long, D.A. Weinberger, K.M. Wilcoxen, M.R. Ghadiri, Nature 412 (2001) 452–455;
(e) C. Valery, M. Paternostre, B. Robert, T. Gulik-Krzywicki, T. Narayanan, J. Dedieu, G. Keller, M. Torres, R. Cherif-Cheikh, P. Calvo, F. Artzner, Proc. Natl. Acad. Sci. USA 100 (2003) 10258–10262.

[4] (a) J.B. Matson, R.H. Zha, S.I. Stupp, Curr. Opin. Solid State Mater. Sci. 15 (6) (2011) 225–235;
(b) S. Santoso, W. Hwang, H. Hartman, S. Zhang, Nano Lett. 2 (7) (2002) 687–691;
(c) H. Cui, T. Muraoka, A.G. Cheetham, S.I. Stupp, Nano Lett. 9 (3) (2009) 945–951.

[5] (a) A.P. Nowak, V. Breedveld, L. Pakstis, B. Ozbas, D.J. Pine, D. Pochan, T.J. Deming, Nature 417 (2002) 424–428;
(b) S. Zhang, D.J. Alvarez, M.V. Sofroniew, T.J. Deming, Biomacromolecules 16 (2015) 1331–1340;
(c) J. Sun, P. Černoch, A. Völkel, Y. Wei, J. Ruokolainen, H. Schlaad, Macromolecules 49 (2016) 5494–5501.

[6] (a) H. Zeng, M.E. Johnson, N.J. Oldenhuis, T.N. Tiambeng, Z. Guan, ACS Cent. Sci. 1 (2015) 303–312;
(b) K.T. Al-Jamal, W.T. Al-Jamal, J.T.-W. Wang, N. Rubio, J. Buddle, D. Gathercole, M. Zloh, K. Kostarelos, ACS Nano 7 (3) (2013) 1905–1917.

[7] M. Reches, E. Gazit, Science 300 (2003) 625–627.

[8] (a) L. Adler-Abramovich, M. Reches, V.L. Sedman, S. Allen, S.J.B. Tendler, E. Gazit, Langmuir 22 (2006) 1313–1320;
(b) N. Kol, L. Adler-Abramovich, D. Barlam, R.Z. Shneck, E. Gazit, I. Rousso, Nano Lett. 5 (2005) 1343–1346.

[9] Y. Song, S.R. Challa, C.J. Medforth, Y. Qiu, R.K. Watt, D. Peña, J.E. Miller, F. van Swol, J.A. Shelnutt, Chem. Commun. (2004) 1044–1045.

[10] (a) A. Mahler, M. Reches, M. Rechter, S. Cohen, E. Gazit, Adv. Mater. 18 (2006) 1365–1370;
(b) V. Jayawarna, M. Ali, T.A. Jowitt, A.F. Miller, A. Saiani, J.E. Gough, R.V. Ulijn, Adv. Mater. 18 (2006) 611–614;
(c) R. Ischakov, L. Adler-Abramovich, L. Buzhansky, T. Shekhter, E. Gazit, Bioorg. Med. Chem. 21 (2013) 3517–3522.

[11] X. Yan, Q. He, K. Wang, L. Duan, Y. Cui, J. Li, Angew. Chem., Int. Ed. 46 (2007) 2431–2434.

[12] (a) R. Roytman, L. Adler-Abramovich, K.S.A. Kumar, T.-C. Kuan, C.-C. Lin, E. Gazit, A. Brik, Org. Biomol. Chem. 9 (2011) 5755–5761;
(b) N. Gour, A.K. Barman, S. Verma, J. Pept. Sci. 18 (2012) 405–412.
[13] P. Kumaraswamy, R. Lakshmanan, S. Sethuraman, U.M. Krishnan, Soft Matter 7 (2011) 2744–2754.
[14] (a) E.D. Bosne, A. Heredia, S. Kopyl, D.V. Karpinsky, A.G. Pinto, A.L. Kholkin, Appl. Phys. Lett. 102 (2013) (073504-1);
(b) D.B. Rasale, S. Biswas, M. Konda, A.K. Das, RSC Adv. 5 (2015) 1529–1537;
(c) T. Heehan, T. Ok, J. Kim, D.O. Shin, H. Ihee, H.S. Lee, S.O. Kim, Small 6 (8) (2010) 945–951.
[15] P. Tamamis, L. Adler-Abramovich, M. Reches, K. Marshall, P. Sikorski, L. Serpell, E. Gazit, G. Archontis, Biophys. J. 96 (2009) 5020–5029.
[16] (a) Y. Mazor, S. Gilead, I. Benhar, E. Gazit, J. Mol. Biol. 322 (2002) 1013–1024;
(b) V. Moretto, M. Crisma, G.M. Bonora, C. Toniolo, H. Balaram, P. Balaram, Macromolecules 22 (1989) 2939–2944.
[17] (a) J.S. Nowick, E.M. Smith, M. Pairish, Chem. Soc. Rev. 25 (1996) 401–415;
(b) C. Perez-Iratxeta, M.A. Andrade-Navarro, BMC Struct. Biol. 8 (2008) 25.
[18] (a) A. Ali, M. Kamra, S. Roy, K. Muniyappa, S. Bhattacharya, Chem. Asian J. 11 (2016) 2542–2554;
(b) S.U. Rehman, Z. Yaseen, M.A. Husain, T. Sarwar, H.M. Ishqi, M. Tabish, PLoS ONE 9 (4) (2014) e93913;
(c) A. Kunwar, E. Simon, U. Singh, R.K. Chittela, D. Sharma, S.K. Sandur, I.K. Priyadarsini, Chem. Biol. Drug Des. 77 (2011) 281–287;
(d) B.K. Sahoo, K.S. Ghosh, R. Bera, S. Dasgupta, J. Chem. Phys. 351 (2008) 163–169;
(e) M. Sirajuddin, S. Ali, A. Badshah, J. Photochem. Photobiol. B: Biol. 124 (2013) 1–19;
(f) H. Li, L. Rothberg, Proc. Natl. Acad. Sci. USA 101 (99) (2004) 14036–14039;
(g) M. Rahban, A. Divsalar, A.A. Saboury, A. Golestani, J. Phys. Chem. C 114 (2010) 5798–5803;
(h) L.A. Gearheart, H.J. Ploehn, C.J. Murphy, J. Phys. Chem. B 105 (2001) 12609–12615;
(i) M. Banik, T. Basu, Dalton Trans. 43 (2014) 3244–3259;
(j) G.N. Roviello, D. Musumeci, E.M. Bucci, C. Pedone, Mol. BioSyst. 7 (2011) 1073–1080;
(k) G.N. Roviello, D. Musumeci, RSC Adv. 6 (2016) 63578–63585.
[19] (a) E.J. Gabbay, P.D. Adawadkar, L. Kapicak, S. Pearce, W.D. Wilson, Biochemistry 15 (1) (1976) 152–157;
(b) J.C. Maurizot, G. Boubault, C. Helene, FEBS Lett. 88 (1) (1978) 33–36;
(c) S.Z. Luo, Y.M. Li, W. Qiang, Y.F. Zhao, H. Abe, T. Nemoto, X.R. Qin, H. Nakanishi, J. Am. Soc. Mass Spectrom. 15 (2004) 28–31;
(d) R.C.K. Yang, J.T.B. Huang, S.C. Chien, R. Huang, K.C.G. Jeng, Y.C. Chen, M. Liao, J.R. Wu, W.K. Hung, C.C. Hung, Y.L. Chen, M.J. Waring, L. Sheh, Org. Biomol. Chem. 11 (2013) 48–61.
[20] U. Chaveerach, A. Meenongwa, Y. Trongpanich, C. Soikum, P. Chaveerach, Polyhedron 29 (2010) 731–738.
[21] (a) M.J. Warning, J. Mol. Biol. 13 (1965) 269;
(b) J.-B. Lepecq, C. Paoletti, J. Mol. Biol. 27 (1967) 87–106;
(c) H.L. Wu, W.Y. Li, X.W. He, K. Miao, H. Liang, Anal. Bioanal. Chem. 373 (2002) 163–168;
(d) A. Rajendran, B.U. Nair, Biochim. Biophys. Acta 1760 (2006) 1794–1801;
(e) G. Pratviel, J. Bernadou, B. Meunier, Int. Ed. Engl. 34 (1995) 746–769;
(f) F.Y. Wu, F.Y. Xie, Y.M. Wu, J.I. Hong, J. Fluoresc. 18 (2008) 175–181;
(g) G. Zhang, L. Wang, X. Zhou, Y. Li, D. Gong, J. Agric. Food Chem. 62 (2014) 991–1000.
[22] (a) X. Zhou, G. Zhang, L. Wang, Int. J. Biol. Macromol. 67 (2014) 228–237;
(b) C.V. Kumar, R.S. Turner, E.H. Asunction, J. Photochem. Photobiol. A 74 (1993) 231–238;
(c) G. Zhang, P. Fu, J. Pan, J. Lumin. 134 (2013) 303–309.
[23] Y.T. Sun, H.Q. Zhang, S.Y. Bi, X.F. Zhou, L. Wang, Y.S. Yan, J. Lumin. 131 (2011) 2299–2306.
[24] (a) M. Bodanszky, A. Bodanszky, The Practice of Peptide Synthesis, Springer, New York, 1984, pp. 1–282;
(b) D.B. Rasale, I. Maity, A.K. Das, Chem. Commun. 50 (2014) 8685–8688;
(c) D.B. Rasale, M. Konda, S. Biswas, A.K. Das, Chem. Asian J. 11 (2016) 926–935;
(d) D.B. Rasale, S. Biswas, M. Konda, A.K. Das, RSC Adv. 5 (2015) 1529–1537.
[25] (a) F.M. Freimoser, C.A. Jakob, M. Aebi, U. Tuor, Appl. Environ. Microbiol. 65 (1999) 3227–3229;
(b) K. Bishayee, S. Ghosh, A. Mukherjee, R. Sadhukhan, J. Mondal, A.R. Khuda-Bukhsh, Cell Prolif. 46 (2013) 153–163;
(c) S. Roy, R. Sadhukhan, U. Ghosh, T.K. Das, Spectrochim. Acta Part A: Mol. Biomol. Spectrosc. 141 (2015) 176–184.